FEBS 26172 FEBS Letters 521 (2002) 133–139



# Molecular dynamics simulations revealed $Ca^{2+}$-dependent conformational change of Calmodulin

Yuto Komeiji[a,*], Yutaka Ueno[b], Masami Uebayasi[a]

[a] *IMCB/RICS, National Institute of Advanced Industrial Science and Technology (AIST), Central 6, Tsukuba 305-8566, Japan*
[b] *NRI/CBRC, National Institute of Advanced Industrial Science and Technology (AIST), Central 6, Tsukuba 305-8566, Japan*

Received 3 April 2002; revised 30 April 2002; accepted 2 May 2002

First published online 27 May 2002

Edited by Thomas L. James

**Abstract Molecular dynamics simulations were performed to simulate $Ca^{2+}$-dependent conformational change of calmodulin (CaM). Simulations of the fully $Ca^{2+}$-bound form of CaM (Holo-CaM) and the $Ca^{2+}$-free form (Apo-CaM) were performed in solution for 4 ns starting from the X-ray crystal structure of Holo-CaM. A striking difference was observed between the trajectories of Holo-CaM and Apo-CaM: the central helix remained straight in the former but became largely bent in the latter. Also, the flexibility of Apo-CaM was higher than that of Holo-CaM. The results indicated that the bound $Ca^{2+}$ ions harden the structure of CaM. © 2002 Published by Elsevier Science B.V. on behalf of the Federation of European Biochemical Societies.**

*Key words:* Calmodulin; Molecular dynamics; Computer simulation; Calcium; Conformation; PEACH; GRAPE

## 1. Introduction

Calmodulin (CaM) is a ubiquitous protein that mediates signal transduction via $Ca^{2+}$ ion [1–3]. In this paper, molecular dynamics (MD) simulations of CaM were performed to characterize $Ca^{2+}$-dependent conformational change of the protein.

CaM consists of 148 amino acid residues (Fig. 1A). A molecule of the $Ca^{2+}$-free form of CaM (apocalmodulin (Apo-CaM)) binds four $Ca^{2+}$ ions, and the resultant fully bound form (holocalmodulin (Holo-CaM)) undergoes a conformational change in order to interact with various proteins [3]. It was recently found that Apo-CaM also interacts with some proteins [4], but usually Holo-CaM is the active form in biological systems. In crystal structures, Holo-CaM adopts a dumbbell-like shape ([5,6], Fig. 1B). CaM is divided into three domains: the N-terminal lobe (N-lobe), the C-terminal lobe (C-lobe), and the central helix (Fig. 1). The solution structures of N-lobe and C-lobe of Holo-CaM have been recently solved by nuclear magnetic resonance (NMR) [7], in which the helices in the lobes took a slightly different orientation from the crystal structure. No crystal structure for Apo-CaM is available, but the solution structure has been solved by NMR [8,9].

Bending of the central helix has long been a major issue of the conformation dynamics of CaM because the helix is postulated to play a key role in the target recognition. The central helix is straight in the crystal structure of Holo-CaM (Fig. 1B), but NMR and fluorescence microscopy studies have shown that the central helix is flexible in solution, and that the two lobes move independently [10–12]. Upon binding some target peptides, the central helix in Holo-CaM adopts a bent conformation, as revealed by NMR [13,14] and by X-ray crystallography [15–17]. The solution structure of Apo-CaM determined by NMR [8,9] again showed the flexibility of the helix. Several small angle X-ray scattering (SAXS) experiments have demonstrated that Holo-CaM has a larger gyration radius ($R_g$) than Apo-CaM does, indicating the global elongation of the protein upon $Ca^{2+}$ binding [18–21]. Presumably, this elongation is attributable to the elongation of the central helix. Similar $Ca^{2+}$-dependent elongation was observed in a gel-permeation experiment [22].

The unusual structure of CaM has also drawn attention of computational scientists. Earlier MD simulations of CaM were performed without an explicit solvent (see [2] for a review), but recent MD simulations described below have been conducted in an explicit solvent to realize realistic simulations. Van der Spoel et al. [23] performed an MD simulation of the central helix and observed bending of the helix. Wriggers et al. [24] performed an MD simulation of Holo-CaM and observed unwinding of the central helix. Vigil et al. [25] performed MD of the whole Holo-CaM, the N-lobe of Holo-CaM, and the N-lobe of Apo-CaM in order to characterize the hydrophobic cleft in the N-lobe. Yamaotsu et al. [26] performed an MD simulation of the CaM/Trifluoperazine complex in order to analyze its binding affinity. Yang and Kuckzera [27] performed MD simulations of Holo-CaM with and without the electrostatic cutoff and compared the results. Nevertheless, to our knowledge, no MD simulation of the whole Apo-CaM in explicit solution has been reported in the literature.

In this study we attempted to characterize the effect of $Ca^{2+}$ on the conformational dynamics of CaM. MD trajectories of Holo-CaM (MD-holo) and Apo-CaM (MD-apo) were generated in explicit solution starting from the crystal structure of Holo-CaM. The structure and dynamics of the two trajectories were compared. In particular, the conformation of the central helix was investigated in detail.

## 2. Materials and methods

### 2.1. Generation of MD trajectories

Two MD trajectories, MD-holo and MD-apo, were generated by

*Corresponding author. Fax: (81)-298-61-6012.
*E-mail address:* y-komeiji@aist.go.jp (Y. Komeiji).

*Abbreviations:* CaM, calmodulin; Holo-CaM, holocalmodulin; Apo-CaM, apocalmodulin; MD, molecular dynamics; SAXS, small angle X-ray scattering

0014-5793/02/$22.00 © 2002 Published by Elsevier Science B.V. on behalf of the Federation of European Biochemical Societies.
PII: S0014-5793(02)02853-3

using a software package, 'Program for Energetic Analysis of bio-CHemical molecules' (PEACH, Ver. 2.08 and 3.0A, [28,29]). Simulations were performed on DEC alpha-stations (600 au and 500 au) equipped with MD-GRAPE (ITL MD one, [28]). The computation time required for 1 fs MD was 3.5 s. The AMBER96 force field [30,31] was used to model the protein and $Na^+$ ion. The force parameter of $Ca^{2+}$ ion was taken from [32]. A flexible version of SPC water [33] rather than a rigid one was used to allow all the degree of freedom to evolve in the simulations. The crystal structure of Holo-CaM determined at 1.7 Å resolution [6] (Fig. 1B) was used as the initial structure of the simulations. Hydrogen atoms were added. Amino acid residues missing from the PDB file were excluded from the simulations (see legend to Fig. 1A). In MD-apo, the $Ca^{2+}$ ions were omitted from the simulation. CaM was immersed in a cubic box of water molecules, and the water molecules within 2.8 Å of the protein were deleted. CaM was placed along the diagonal line of the cube to minimize the interaction with the images. $Na^+$ ions sufficient to neutralize the systems were added by replacing some of the water molecules so that the protein–ion electrostatic interaction would be a minimum. The initial configurations thus prepared are represented in Fig. 2. Steepest descent energy minimization was performed for 200 steps, followed by 100 steps of quenched dynamics at a time step of 0.1 fs at 0.1 K. Finally, MD simulations were performed for 4 ns. See Table 1 for further details of the simulation protocol.

The generated trajectories showed a good energetic stability. Namely, the relative fluctuation of the Nose-Hamiltonian, the conservative, was as low as 0.05% for the 0.5–4.0 ns trajectories (not shown). In MD-holo, the $Ca^{2+}$ ions remained close to the ligand atoms of the protein during the simulation; the distance between each ion–ligand pair was mostly shorter than 3 Å (not shown). Thus, MD-holo was regarded as a good model of the $Ca^{2+}$-bound form of CaM.

### 2.2. Analyzes of MD trajectories

The conformational dynamics of the generated trajectories were analyzed by various methods.

Throughout this study, N, CA, and C atoms were regarded as main chain atoms, consistent with Kuboniwa et al. [8]. The root mean square difference (RMSD) between two structures $i$ and $j$ was calculated as follows:

$$\mathrm{RMSD} = \left(1/n \sum_{k=1}^{n} |\boldsymbol{R}_k^i - \boldsymbol{R}_k^j|^2\right)^{1/2}, \quad (1)$$

where $\boldsymbol{R}_k^i$ stands for the coordinate of the $k$-th main chain atom of structure $i$. The summation was performed over all $n$ main chain atoms. The radius of gyration ($R_g$) was calculated as follows:

$$R_g = \left(\sum_{i=1}^{N} m_i \Delta r_i^2 \Big/ \sum_{i=1}^{N} m_i\right)^{1/2}, \quad (2)$$

where $m_i$ and $\Delta r_i$ are the mass and the distance from the centroid of the $i$-th atom of the molecule, respectively. The summations were performed over all $N$ atoms that comprise the molecule. The pair distance distribution function ($P(r)$) was calculated as follows:

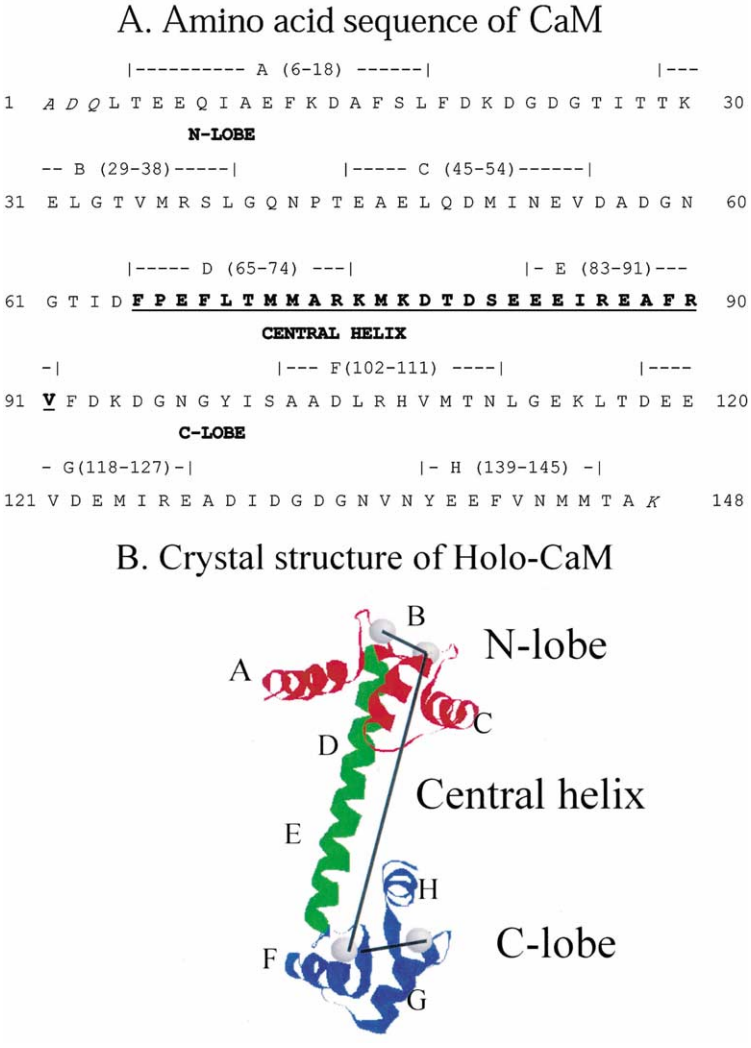


Fig. 1. A: The amino acid sequence of CaM. Amino acid residues missing from the PDB file are shown in italics. CaM consists of N-lobe (aa 4–64), central helix (aa 65–92, underlined), and C-lobe (aa 93–148). Alpha-helices A–H are shown as defined in [8]. B: The crystal structure of Holo-CaM [6]. The VDA defined by the $Ca^{2+}$ ions is shown.

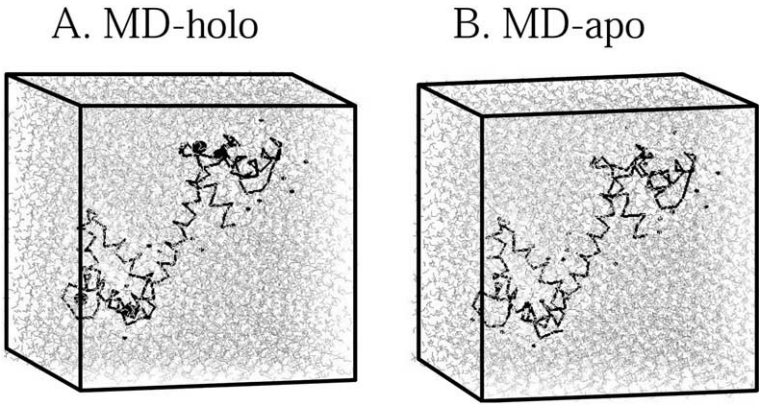


Fig. 2. Initial configurations for MD simulations. The protein was presented in a backbone trace, with $Ca^{2+}$ ions in large balls and $Na^{+}$ ions in small balls.

$$P(r) = \Delta n(r)/n\Delta r \quad (3)$$

where $n$ is the total number of atom pairs in the protein and $\Delta n(r)$ is the number of atom pairs whose distance is between $r-\Delta r/2$ and $r+\Delta r/2$. The axis angle between a pair of alpha-helices ($i$, $j$) was computed as follows [8]. The axis vector $\mathbf{e}_i$ of helix $i$ was obtained as a vector connecting the geometrical center of 10 main chain atoms from the N-terminus of the helix and that of 10 main chain atoms from the C-terminus. The axis angle between helices $i$ and $j$ was obtained as an angle defined by $\mathbf{e}_i$ and $\mathbf{e}_j$. The experimental and simulated structures were visualized by RASMOL 2.6 [34]. Movies of the trajectories were generated by MOSBY [35] and were used to investigate the dynamics.

## 3. Results and discussion

### 3.1. Overall conformational dynamics

The overall conformational change and dynamics of the trajectories were illustrated by showing RMSD and by superimposing the coordinates.

Time-dependent change of RMSD from the initial crystal structure of Holo-CaM is shown for MD-holo and MD-apo (Fig. 3). In MD-holo, RMSD of each domain (N-lobe, C-lobe, and the central helix) was about 2 Å or lower (Fig. 3A), indicating that the local structure of each domain was mostly conserved during the simulation. RMSD of the whole protein fluctuated during MD-holo, indicating the fluctuation of the relative position of each domain. In MD-apo, RMSD of each of the three domains was larger than in MD-holo, and RMSD of the whole protein increased and became as large as 10 Å at the end of the simulation (Fig. 3B).

Next, the conformational dynamics was illustrated by superimposing the coordinates from the 2–4 ns trajectories (Fig. 4). A striking difference was observed between MD-holo and MD-apo. The local domain structures were conserved in MD-holo but not in MD-apo. The global structures deviated in both trajectories, but the deviation was much larger in MD-apo. The main difference between MD-holo and MD-apo was that the central helix was almost straight in the former but was largely bent in the latter. This difference was all the more interesting because the central helix was not in direct contact with the $Ca^{2+}$ ions. Hence, this was one of rare cases in which MD reproduced an allosteric conformational change induced by ions.

### 3.2. Conformation of the central helix

As stated in the introduction (Section 1), the bending of the central helix has been a major issue of CaM. Hence, the remarkable difference in the conformation of the central helix between MD-holo and MD-apo was further analyzed.

Prior to comparison of MD-holo and MD-apo, we ana-

Table 1
Simulation protocol

| | | | |
|---|---|---|---|
| Initial structure | PDB 1CLL [6] | | |
| Force field | Protein and $Na^{+}$: | AMBER96 [30,31] | |
| | $Ca^{2+}$: | Bartolotti et al. [32] | |
| | Water: | Flex SPC [33] | |
| Ensemble | Nose-Hoover [40] | | |
| | 0–9 ps (heating) | 0–300 K (Tau = 0.01 ps) | |
| | 9 ps-4 ns: | 300 K (Tau = 0.5 ps) | |
| Electrostatic interaction | Ewald summation (Epsilon = $3\times10^{-5}$, [29]) | | |
| Integration | RESPA [41] | | |
| Time steps | Bond, angle torsion: | 0.25 fs | |
| | Van der Waals and Ewald-real space: | 2.00 fs | |
| | Ewald-wave number space: | 4.00 fs | |
| Box dimensions | $67\times67\times67$ Å$^3$ | | |
| | (the shortest distance between wall and protein: 8 Å) | | |
| Number of atoms | | MD-holo | MD-apo |
| | Protein | 2 202 | 2 202 |
| | $Na^{+}$ | 15 | 23 |
| | $Ca^{2+}$ | 4 | 0 |
| | Solvent | 25 893 | 25 866 |
| | Total | 28 114 | 28 091 |

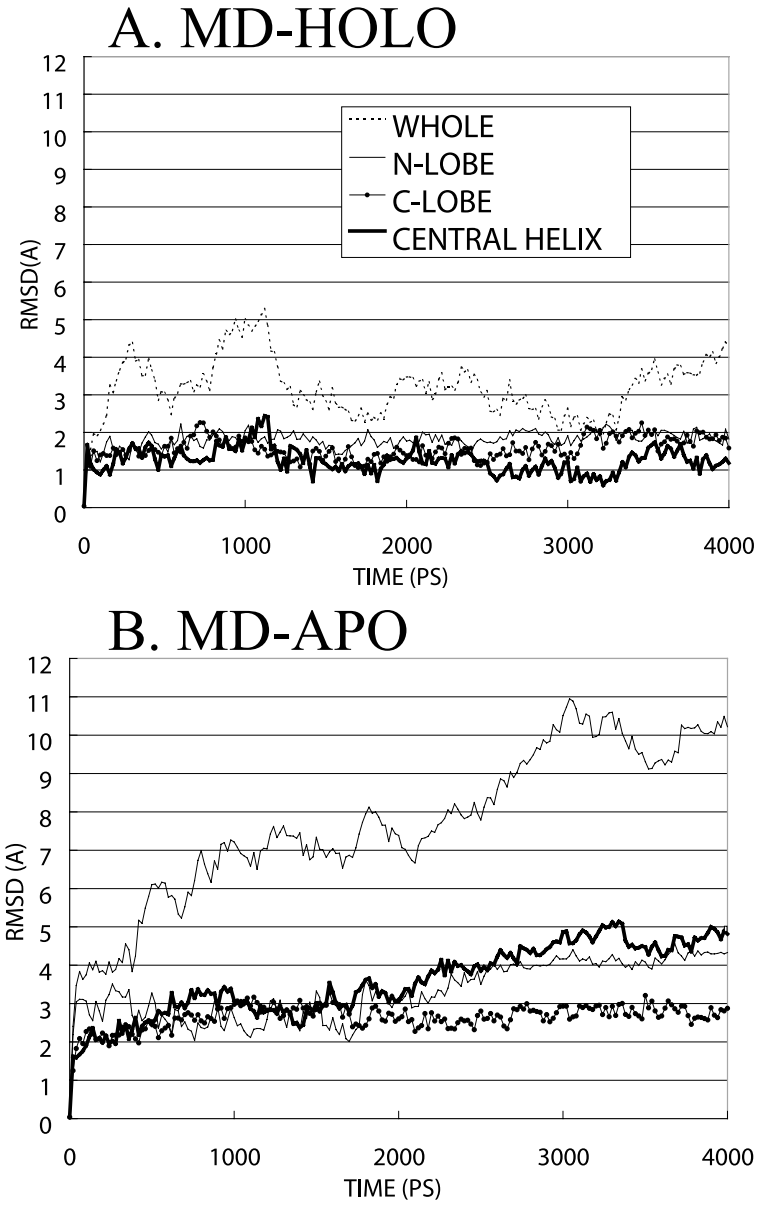


Fig. 3. Time evolution of RMSD between the crystal and simulated structures calculated by Eq. 1.

lyzed a virtual dihedral angle (VDA) defined by the four $Ca^{2+}$ atoms [36] (Fig. 1B) for MD-holo to characterize the inter-domain orientation. Presumably, the value of the VDA is largely influenced by the conformation of the central helix.

The time evolution of the VDA in MD-holo is presented in Fig. 5. The VDA became −90° for the first 1 ns and became gradually to −160° by 4 ns. This result was similar to Yang et al. [27] but was different from Wriggers et al. [24] and Vigil et al. [25]; in the latter two simulations, the VDA gradually became −190° and was stable for the rest of the simulation. The discrepancy among the four simulations of Holo-CaM including ours could be attributable to the short simulation time. All of the four simulations covered a time scale of only a few nanoseconds, which is insufficient for the characterization of the global dynamics of CaM. Also, the periodic boundary ([25,27] and this study) or the wall of the water droplet [24] could have some artifact on the motion of the protein. However, all the simulations of Holo-CaM in solution clearly indicated the rotational freedom around the central helix.

Next, the time course of the bending angle between helices D and E was investigated to compare the tendency of the central helix to bend between MD-holo and MD-apo (Fig. 6). Clearly, the helix was largely bent in MD-apo. The central helix was also largely bent in a 3 ns MD of the isolated central helix [23]. The helix had a tendency to bend also in MD-holo (Fig. 6), showing that MD-holo was not in conflict with the spectroscopic data indicating its flexibility [10,12,32]. Similarly, in a simulation of Holo-CaM by Wriggers et al. [24], the central helix was unwound in the middle. However, the bending or unwinding was not as extensive as in MD-apo in all the MD simulations of the solvated Holo-CaM so far reported ([23–25,27] and MD-holo of this study).

In the NMR structures of Apo-CaM, the central helix did not adopt a static structure such as that seen in MD-apo;

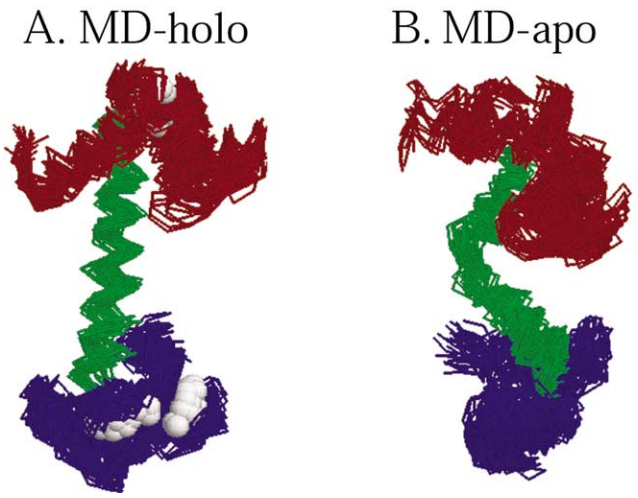


Fig. 4. Superimposed snapshots from MD-holo (A) and MD-apo (B). Snapshots were sampled every 0.1 ns from the 0.5–4 ns trajectories.

rather, it was an ensemble of many conformers [8,9]. This fact suggested that the bent structure seen in MD-apo was trapped in a local minimum in the energy landscape. Still, the difference between MD-holo and MD-apo has revealed an allosteric effect of the bound $Ca^{2+}$ ions on the conformation of the central helix.

Thus, a large conformational change upon $Ca^{2+}$-binding was observed. Nonetheless, we must consider the force field dependence of the MD results. Several recent studies demonstrated that current force field parameter sets give quite different results in folding or conformational dynamics [37–39]. The AMBER96 force field, which we used, has been shown to favor an extended conformation over a compact one in certain circumstances. Also, the dependence of the solvent model on the protein dynamics has not yet been thoroughly analyzed. In this regard, we cannot deny the possibility of the force field dependence of the minute structural features of the simulated trajectories, for example, arrangement of the helices and orientation of the domains.

Nevertheless, we think that the conformational difference of the central helix observed between MD-holo and MD-apo should be essentially reliable because of several reasons. First, the conformation of the central helix seen in MD-holo was similar to the previous simulations of Holo-CaM obtained under different force field sets and solvent models [23–25,27]. Namely, the helix was on average straight but was apt to bend a little. Secondly, the largely bent conformation of the central helix seen in MD-apo was also obtained in an MD trajectory of the isolated helix obtained under a different force field set [23]. Thirdly, the shrinkage of CaM upon release of $Ca^{2+}$ was consistent with SAXS experiments (see Section 3.3).

In summary, considering the current simulations and previous ones, the central helix is inclined to bend in nature. Nevertheless, in Holo-CaM, the bound $Ca^{2+}$ ions prevent the central helix from extensive bending.

### 3.3. Comparison with SAXS – $R_g$ and $P(r)$

The conformation of CaM in solution has been analyzed by a number of SAXS experiments, which have given the $R_g$ and $P(r)$ of various forms of CaM in solution. The $R_g$ and $P(r)$ were computed from the MD trajectories and compared with the available SAXS results.

The experimental and computed $R_g$ values are listed in Table 2. The experimental values differ depending on the papers, but all of the SAXS results showed that $R_g$ of Holo-CaM is larger than that of Apo-CaM. The relative difference in $R_g$ was also seen between MD-holo and MD-apo. Thus, the simulations reproduced the $Ca^{2+}$-dependent elongation of the CaM molecule observed in SAXS experiments.

Then, the $P(r)$ functions were drawn for MD-holo, MD-apo, and the crystal structure (Fig. 7). $P(r)$ of the crystal structure had a relatively sharp peak at 17 Å and a broad one at 40 Å, reflecting the dumbbell-like shape. The former represents the intra-domain distance distribution while the latter represents the inter-domain distance distribution [18]. The shape of $P(r)$ in MD-holo was similar to that of the crystal structure, but $P(r)$ of MD-apo was different. The sec-

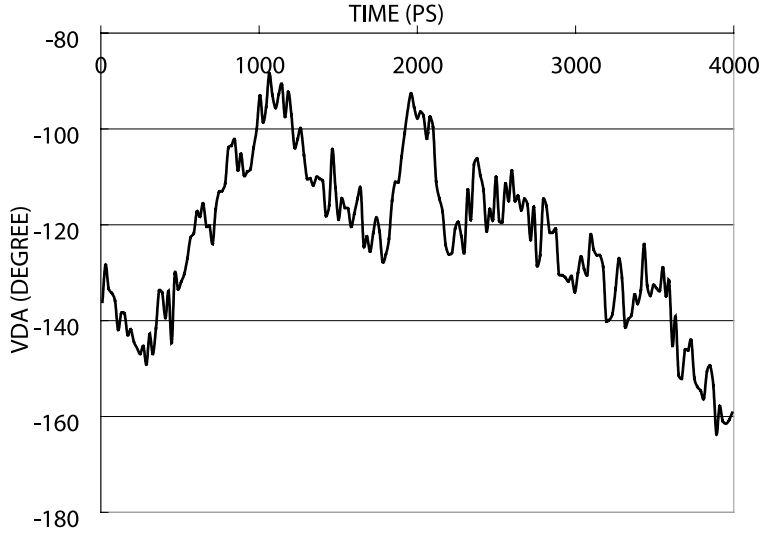


Fig. 5. Time evolution of the bending angle of the central helix. The angle between helices D and E was plotted.

Table 2
$R_g$ values (Å) for CaM determined by experiments and MD

| | Holo-CaM | Apo-CaM | $R_g$(holo)–$R_g$(apo) |
|---|---|---|---|
| SAXS[a] | | | |
| Seaton et al. [18] | 21.5 ± 0.2 | 20.6 ± 0.6 | 0.9 |
| Heidorn and Trewhella [19] | 21.3 ± 0.2 | 19.6 ± 0.1 | 1.7 |
| Matsushima et al. [20] | 21.5 ± 0.3 | 20.9 ± 0.3 | 0.6 |
| Kataoka et al. [21] | 20.2 ± 0.1 | 19.5 ± 0.1 | 0.7 |
| X-ray crystallography | | | |
| Chattopadhyaya et al. [6] | 21.9 | | |
| MD | | | |
| Wriggers et al. [24] | 22 ± 1 | | |
| This study[b] | 21.9 ± 0.4 | 20.4 ± 0.4 | 1.5 |

[a]For SAXS results, only those papers examining both Holo and Apo forms are listed.
[b]Computed by Eq. 2.

ond peak almost disappeared and became a shoulder in MD-apo.

The $P(r)$ functions of both Apo-CaM and Holo-CaM obtained by SAXS were different from that of the crystal structure [18,20]. In SAXS, the second peak was not observed, and only a shoulder was present around 40 Å. The difference between Holo-CaM and Apo-CaM was small, but the first peak was higher in the latter and the shoulder was higher in the former. The SAXS results suggested that some portion of the CaM molecules in solution adopt a fairly globular shape, with N-lobe and C-lobe much closer to each other than in the crystal, and that the relative population of such a globular conformation is slightly larger in Apo-CaM than in Holo-CaM. Therefore, $P(r)$ of MD-apo was consistent with that obtained by SAXS. Though the shape of $P(r)$ of MD-holo was not precisely consistent with that by SAXS, the experimental difference in the relative height of the peaks between Apo-CaM and Holo-CaM was qualitatively reproduced by MD.

Thus, the MD trajectories were consistent with the $Ca^{2+}$-induced elongation of the CaM molecule observed in SAXS experiments. This global conformational change should be attributable to the bending of the central helix discussed in Section 3.2.

## 4. Conclusion

In this study, MD simulations of Holo-CaM and Apo-CaM were performed in solution starting from the X-ray structure of Holo-CaM. In MD-holo, the conformation remained fairly close to the X-ray structure, but that in MD-apo was quite different.

The MD trajectories have shown several important aspects of this molecule.

1. A large conformational difference exists between Holo-CaM and Apo-CaM.
2. The bound $Ca^{2+}$ ions stabilize and harden the structure of Holo-CaM.
3. The central helix is apt to bend, but the bound $Ca^{2+}$ ions interfere with extensive bending via an allosteric effect.

In biological systems, Apo-CaM is activated by $Ca^{2+}$ ions, and the resultant complex, namely Holo-CaM, activates various enzymes. Our study suggested that the main role of the $Ca^{2+}$ ions is fixation of the conformation of the protein. Namely, without the $Ca^{2+}$ ions, the protein should be too soft to make specific interactions with other proteins. The current study has thus partly reproduced one of the fundamental roles of ions in biological reactions.

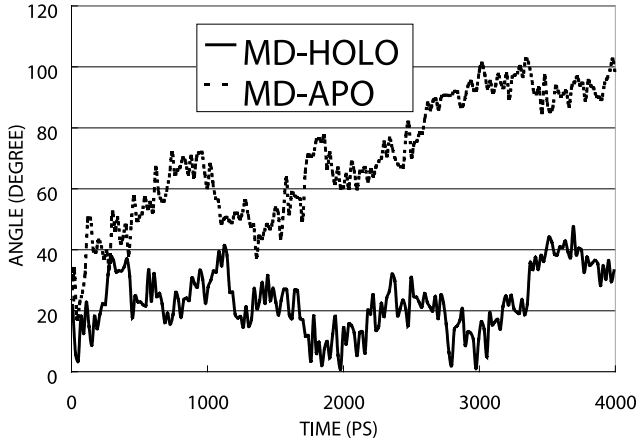


Fig. 6. Time evolution of the VDA in MD-holo. See Fig. 1B for a visual definition of the VDA.

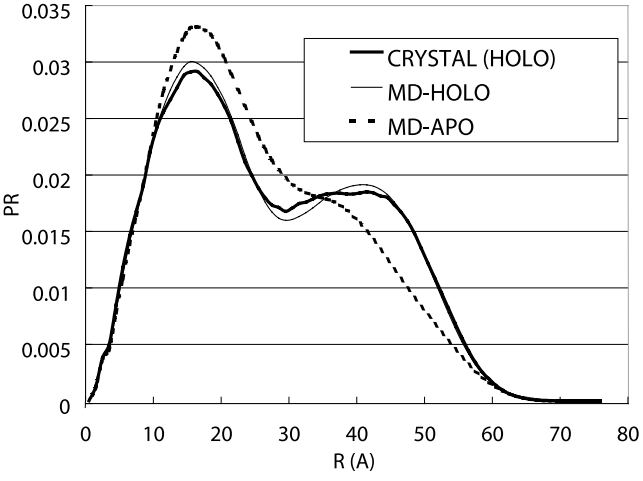


Fig. 7. The $P(r)$ functions for the crystal structure of Holo-CaM and 2–4 ns MD trajectories calculated by Eq. 3.

*Acknowledgements:* We thank Dr. James Chou of NIH for sending us the NMR structure of Holo-CaM prior to publication. We are grateful to Dr. Tadashi Nemoto of AIST for helpful discussions.

## References

[1] Cohen, P. and Klee, C.B. (1988) Calmodulin, Elsevier, Amsterdam.
[2] Weinstein, H. and Mehler, E. (1994) Annu. Rev. Physiol. 56, 213–236.
[3] Crivici, A. and Ikura, M. (1995) Annu. Rev. Biophys. Biomol. Struct. 24, 85–116.
[4] Jurado, L.A., Chockalingam, P.S. and Jarret, H.W. (1999) Physiol. Rev. 79, 661–682.
[5] Babu, Y.S., Bugg, C.E. and Cook, W.J. (1988) J. Mol. Biol. 204, 191–204.
[6] Chattopadhyaya, R., Meador, W.E., Means, A.R. and Quiocho, F.A. (1992) J. Mol. Biol. 228, 1177–1192.
[7] Chou, J.J., Li, S., Klee, C.B. and Bax, A. (2001) Nat. Struct. Biol. 8, 990–997.
[8] Kuboniwa, H., Tjandra, N., Grzesiek, S., Ren, H., Klee, C.B. and Bax, A. (1995) Nat. Struct. Biol. 2, 768–776.
[9] Zhang, M., Tanaka, T. and Ikura, M. (1995) Nat. Struct. Biol. 2, 758–767.
[10] Ikura, M., Spera, S., Barbato, G., Kay, L.E., Krinks, M. and Bax, A. (1991) Biochemistry 30, 9216–9228.
[11] Barbato, G., Ikura, M., Kay, L.E., Pastor, R.W. and Bax, A. (1992) Biochemistry 31, 5269–5278.
[12] Sun, H., Yin, D. and Squires, T.C. (1996) Biochemistry 38, 12266–12279.
[13] Ikura, M., Clore, G.M., Gronenborn, A.M., Zhu, G., Klee, C.B. and Bax, A. (1992) Science 256, 632–638.
[14] Osawa, M., Tokumitsu, H., Swindells, M.B., Kurihara, H., Orita, M., Shibanuma, T., Furuya, T. and Ikura, M. (1999) Nat. Struct. Biol. 6, 819–824.
[15] Meador, W.E., Means, A.R. and Quiocho, F.A. (1992) Science 257, 1251–1255.
[16] Meador, W.E., Means, A.R. and Quiocho, F.A. (1993) Science 262, 1718–1721.
[17] Schumacher, M.A., Rivard, A., Bachinger, H.P. and Adelmen, J.P. (2001) Nature 410, 1120–1124.
[18] Seaton, B.A., Head, J.F., Engelman, D.M. and Richards, F.M. (1985) Biochemistry 24, 6740–6743.
[19] Heidorn, D.B. and Trewhella, J. (1988) Biochemistry 27, 909–915.
[20] Matsushima, N., Izumi, Y., Matsuo, T., Yoshino, H., Ueki, T. and Miyake, Y. (1989) J. Biochem. 105, 883–887.
[21] Kataoka, M., Head, J.F., Seaton, B.A. and Engelman, D.M. (1989) Proc. Natl. Acad. Sci. USA 86, 6944–6948.
[22] Sorensen, B.R. and Shea, M.A. (1996) Biophys. J. 71, 3407–3420.
[23] Van Der Spoel, D., De Groot, B.L., Hayward, S., Berendsen, H.J.C. and Vogel, H.J. (1996) Protein Sci. 5, 2044–2053.
[24] Wriggers, W., Mehler, E., Pitici, F., Weinstein, H. and Schulten, K. (1998) Biophys. J. 74, 1622–1639.
[25] Vigil, D., Gallagher, S.C., Trewhella, J. and Garcia, A.E. (2001) Biophys. J. 80, 2082–2092.
[26] Yamaotsu, N., Suga, M. and Hirono, S. (2001) Biopolymers 58, 410–421.
[27] Yang, C., Jas, G.S. and Kuczera, K. (2001) J. Biomol. Struct. 19, 247–271.
[28] Komeiji, Y., Uebayasi, M., Takata, R., Shimizu, A., Itsukashi, K. and Taiji, M. (1997) J. Comp. Chem. 18, 1546–1563.
[29] Komeiji, Y. and Uebayasi, M. (1999) Mol. Simul. 21, 303–324.
[30] Cornell, W.D., Cieplak, P., Bayly, C.I., Gould, I.R., Merz, K.M., Ferguson, D.M., Spellmeyer, D.C., Fox, T., Caldwell, J.W. and Kollman, P.A. (1995) J. Am. Chem. Soc. 117, 5179–5197.
[31] Kollman, P.A., Dixon, R., Cornell, W., Fox, T., Chipot, C. and Phorille, A. (1997) in: Computer Simulation of Biomolecular Systems (Van Gunsteren et al., Eds.), Vol. 3, pp. 83–96, Kluwer/Escom, Dordrecht.
[32] Bartolotti, L.J., Pedersen, L.G. and Charifson, P.S. (1991) J. Comput. Chem. 12, 1125–1128.
[33] Dang, L.X. and Pettitt, B.M. (1987) J. Phys. Chem. 91, 3349–3354.
[34] Sayle, R.E. and Milnerwhite, E.J. (1995) Trends Biochem. Sci. 20, 374–376.
[35] Ueno, Y. and Asai, K. (2002) J. Mol. Graph. Model. 20, 411–413.
[36] Pascal-Ahuir, J.-L., Mehler, E. and Weinstein, H. (1991) Mol. Eng. 1, 231–247.
[37] Ono, S., Nakajima, N., Higo, J. and Nakamura, H. (2000) J. Comput. Chem. 21, 748–762.
[38] Higo, J., Ito, N., Kuroda, M., Ono, S., Nakajima, N. and Nakamura, H. (2001) Protein Sci. 10, 1160–1171.
[39] Sanbonmatsu, K.Y. and Garcia, A.E. (2002) Proteins 46, 225–234.
[40] Nose, S. (1991) Prog. Theor. Phys. 103 (Suppl.), 1–46.
[41] Tuckerman, M., Berne, B.J. and Martyna, G.J. (1992) J. Chem. Phys. 97, 1990–2001.